# A Comparative Study Of Simulation Tools To Model The Solar Irradiation On Building Façades

**Martin Thebault[1], Benjamin Govehovitch[2], Karine Bouty[1], Cyril Caliot[3], Raphaël Compagnon[4], Gilles Desthieux[5], Matteo Formolli[6], Stéphanie Giroux-Julien[2], Victor Guillot[5], Ellis Herman[7], Jérôme H. Kämpf[8], Jouri Kanters[9], Gabriele Lobaccaro[10], Christophe Ménézo[1], Giuseppe Peronato[8], and Arnkell Jonas Petersen[11]**

[1] University Savoie Mont-Blanc, CNRS, LOCIE UMR 5271, 73376 Le Bourget-du-Lac, France
[2] Univ Lyon, UCBL, INSA Lyon, CNRS, CETHIL, UMR5008, 69266 Villeurbanne France
[3] Universite de Pau et des Pays de l'Adour, E2S UPPA, CNRS, LMAP, Pau, France
[4] Haute Ecole d'Ingénierie et d'Architecture de Fribourg, 1700 Fribourg, Switzerland
[5] Haute école du Paysage d'Ingénierie et d'Architecture de Genève (Hepia), Institute for Landscaping Architecture Construction and Territory (inPACT), University of Applied Sciences Western Switzerland, 1202 Geneva, Switzerland
[6] Department of Architecture and Technology, Faculty of Architecture and Design, Norwegian University of Science and Technology NTNU, Trondheim, Norway
[7] Spacemaker - Autodesk
[8] Idiap Research Institute, 1920 Martigny, Switzerland
[9] Division of Energy & Building Design, Department of Architecture and the Built Environment, Lund University, 221 00 Lund, Sweden
[10]Department of Civil and Environmental Engineering, Faculty of Engineering, Norwegian University of Science and Technology NTNU, Trondheim, Norway
[11] Erichsen & Horgen, 0484 Oslo, Norway

**Abstract**

This paper presents a comparison among eight tools commonly used to evaluate the solar irradiation in urban environments. The focus is on the vertical surfaces (i.e., façades). The analysed tools have a large range of applications, from detailed microclimate studies to large-scale irradiation modelling. The benchmark tests consist of simulations using two conceptual urban designs. Two representative winter and summer days are defined. The results, obtained for the modelling of the shortwave irradiance received on the façades, are discussed together with the observed differences. This work provides an overview of some of the available tools, their features, similarities, and differences as well as a comparison of the modelled solar irradiation. This work is conducted in the framework of IEA SHC Task 63 "Solar Neighborhood Planning" where experts from five countries, in six universities, two companies and one research institute have been engaged.

*Keywords: comparative study, vertical façades, solar irradiation, numerical tools*

## 1. Introduction

The use of solar energy in urban environment is considerably spreading IRENA (2019)**.** In this context, it is crucial to model the solar irradiance in cities, which are characterized by complex built environments and related complex urban phenomena such as overshading effects and solar mutual inter-buildings and ground reflections. Indeed, the knowledge of the solar irradiance is important for passive and active uses of solar energy. In urban environment, photovoltaic (PV) systems installed on roofs represent most of the existing installed capacity. However, the integration of PV systems on façades becomes increasingly appealing due to a drop in PV technology prices and the large availability of vertical surfaces for energy production. Moreover, the production profile of PV components installed on façades is often shifted compared to roof-integrated PV modules, which allows for smoothening the electric production during the day Freitas and Brito (2019). An increasing number of simulation tools have now the ability to model solar irradiance in urban environments. However, it is crucial to understand how these tools work as well as what their main


doi:10.18086/swc.2021.38.04 Available at http://proceedings.ises.org

features, level of accuracy, similarities**,** and differences are. To this end, this work presents a comparative study of results from ten simulation tool**s** with a focus on the vertical fa**ç**ades.

## 2. Methodology

To compare results obtained with the selected tools, different levels of complexity will be analysed. Three scenarios have been considered. In the first scenario (i.e. Unshaded roof and Unshaded façade) we will consider the case of an unshaded building, while in the second scenario (i.e. Homogenous district) we will consider the case of a district with a regular distribution of same-size buildings and in the final scenario (i.e. Heterogeneous district) the case of a more random distribution of buildings with different heights.

### 2.1. Geometry

The homogeneous district presented in Figure 1 (a) is composed of three rows of three buildings. The buildings have identical heights and they are vertically and horizontally aligned. The heterogeneous district (b) is composed of non-aligned buildings with various heights. Each of these districts is composed of nine buildings with a footprint of $20 \times 20\ m^2$. Each building is composed of $N_f$ floors, with every floor being 3 m high. For example, a building with $N_f = 5$ will be 15 m high. For each district, the focus is on the central building, coloured in red in Figure 1.

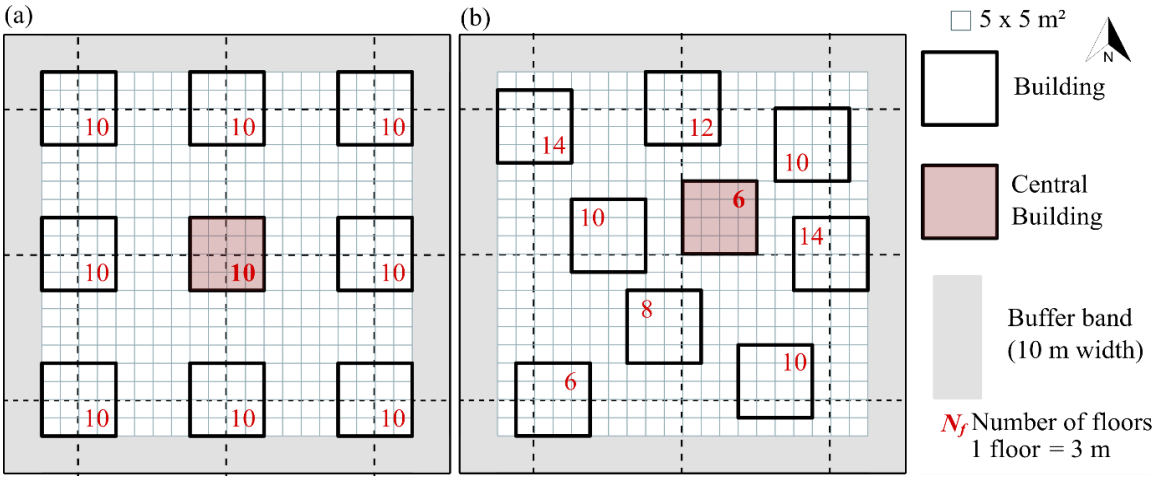


**Figure 1 Theoretical district geometries: (left) homogeneous district, (right) heterogeneous district. North is oriented upward.**

Note that despite these two districts having distinct geometry, they have been designed to share similar common urban form indicators Natanian et al. (2019). These indicators are summarized in Table 1.

**Table 1: Urban morphology indicators of the districts**

| Indicator | Definition | Value |
|---|---|---|
| Shape factor | Ratio between building envelope surface and building volume | 0.23 |
| Floor area ratio | Ratio between building gross floor area and site area | 2.5 |
| Site Coverage | Ratio between building footprint and site area | 0.25 |
| Average Building Height | Average height of buildings in an urban model (m) | 30 |
| | Albedo and reflection coefficients | 0.2 |

### 2.2. Weather data

For the weather inputs, data from the Meteonorm database corresponding to the location of Geneva, Switzerland

(latitude: 46.2044° N, longitude: 6.1432° E), has been used. This database provides hourly data weather conditions (e.g., irradiation, wind speed, temperature, and humidity). The analyses were conducted on two days, one in August and one in February, corresponding to typical summer and winter conditions. The investigated days are obtained from an average of the weather conditions for the considered month. For example for weather input $W$ (e.g. direct irradiation, wind speed, temperature), the monthly averaged weather inputs are obtained by:

$$W_m(h) = \frac{1}{N_m}\sum_{k=1}^{N_m} W_k(h) \qquad \text{(eq. 1)}$$

where the subscript $m$ corresponds to the considered month (here February or August), $N_m$ corresponds to the number of days in the month and $h$ is the hourly time step. Finally, the sun paths corresponding to the days of the 15th of February and the 16th of August will be considered as suggested by Klein (1977). The weather file contains the direct normal irradiance $B_n$, the horizontal sky diffuse irradiance $D_h$ and the global horizontal irradiance $G_h$ .

## 2.3. Temporal and spatial resolution

To conduct the comparative study, all tools must follow the same settings which include the geometry, the thermal properties (i.e. reflection coefficient), the weather and the temporal and spatial resolutions. Not all tools can achieve the same resolution, as some tools focus on district/city scale in which spatial and temporal resolutions are usually much coarser than in tools working at the room/building level.

For the spatial resolution, the surface of the selected building (i.e. central building) is divided into an analysis grid of 1 m² resolution. Results are collected at an hourly resolution. These spatial and temporal resolutions allow for all considered tools to achieve simulations within a reasonable computational time. Higher spatial resolutions would be necessary if superstructure elements were present Peronato et al. (2018), but for these simple geometries and flat surfaces, a 1-m² resolution is sufficient Govehovitch et al. (2021). Regarding the temporal resolution, most of the studies at the district scale consider yearly or monthly cumulated energy. Therefore, an hourly resolution is here sufficient for the aim of this study.

## 2.4. Output solar irradiance and insolation

As mentioned, results are collected at an hourly resolution. From here two solutions are possible:

1. The results are provided as an instantaneous snapshot at the required time, in this case it would correspond to a distribution of the radiative heat flux (in W/m²) on the surfaces of the selected building.
2. Provide an integration of the irradiance during a certain period, here an hour. In this case the result is an energy (in W.s/m$^2$, or in Wh/m$^2$ in the case of solar energy, 1 Wh being the integration of 1 W for one hour). This is sometimes referred to as the ‘insolation’ or ‘irradiation’.

Depending on the adaptability of the tools, it is not always possible to select the required output as some tools impose the output results, either as an irradiance or as an hourly insolation. In what follows, results are presented in terms of irradiation. In the case the tool provides an irradiance, this irradiance is considered as constant for one hour, which leads to an hourly insolation/irradiation. Therefore, the results of this study will be provided in Wh/m$^2$.

## 2.5. Investigated tools

The investigated tools for the comparison study are listed in Table 2. The tools have been selected according to the individual experiences gained by the experts (i.e. co-authors) within the International Energy Agency – Solar Heating and Cooling programme Task 63 “Solar Neighborhood Planning” (Task 63).”.

**Table 2 List and features of the investigated tools in the comparison study**

| Tool Name | Code access | Radiation method | Simulation Engine | Diffuse model |
|---|---|---|---|---|
| Solar Cadastre of Geneva (CaS) | Closed | Radiosity | Own Engine | Hay |
| CitySim (CiS) | Open | Radiosity | SRA | Perez |
| De Luminae (DL) | Closed | Ray-tracing | Radiance | Perez |
| Diva For Rhino (Diva) | Closed | Ray-tracing | Daysim | Perez |
| ENVI-met (EM) | Closed | Radiosity | Own engine | Isotropic |
| Honeybee (HB) | Open | Ray-tracing | Radiance | Perez |
| htrdr-ModRadUrb (ht) | Open | Monte-Carlo (Ray-tracing) | htrdr-0.6.1 | Isotropic |
| Indalux (Ind) | Open | Ray-tracing | Radiance | Perez |
| Ladybug (LB) | Open | Ray-tracing | Radiance | Perez |
| Spacemaker (SP) | Closed | Ray-tracing | Own Engine | Simple Sandia Sky |

- CadSol

The Solar cadastre of Geneva is a geographic information system (GIS) originally created at the Haute école du Paysage d'Ingénierie et d'Architecture de Genève (Hepia), and further developed though different project as it is now within the G2Solaire, INTERREG V project. This tool provides an estimate of the irradiation received on the roofs of the Greater Geneva agglomeration (2000 km²). A detailed presentation of the tool can be found in Desthieux et al. (2018).

- CitySim

CitySim was initially developed at EPFL (the Swiss Federal Institute of Technology in Lausanne) and the solver is currently maintained and further developed as an open-source tool at the Idiap Research Institute. A Graphical User Interface (CitySim Pro) is released as commercial software by Kaemco LLC. CitySim is a complete tool for dynamic urban energy simulation, including solar potential, building energy demand, district heating networks and outdoor comfort. For solar radiation, it includes the Simplified Radiosity Algorithm by Robinson and Stone (2005) and the Perez All-Weather model for the sky radiance distribution.

- DL-Ligth

DL-Light is the software suite developed by De Luminæ to help the evaluation of the intake and distribution of natural light in architectural and urban spaces. It is based on Radiance ([DL-LIGHT]).

- Diva

DIVA-for-Rhino is a highly optimised daylighting and energy modelling plug-in for Rhinoceros. This software uses ray-tracing and light-backwards algorithms based on the physical behaviour of light in a 3D volumetric model. For hourly solar radiation, the Daysim interface is used Reinhart and Walkenhorst (2001).

- ENVI-met

ENVI-met is a software aiming at simulating the urban microclimate by taking into consideration all the complex phenomena that occur in an urban environment. It is based on coupled balance equations (including those of mass, momentum, and energy). This involves taking the built and natural environment into account Simon et al. (2021).

- htrdr

htrdr-ModRadUrb is a numerical tool developed from the free and open-source software htrdr-0.6.1 ([htrdr].) that implements a Backward Monte-Carlo algorithm to compute longwave or shortwave radiative intensities in urban geometry by solving the monochromatic radiative transfer equation in the semi-transparent atmosphere with

Lambertian or specular surfaces. The htrdr-ModRadUrb tool used for this specific study includes a uniform and isotropic model of the sky for the computation of shortwave radiative fluxes as well as grey and Lambertian surfaces.

- HoneyBee

Honeybee is an open-source plug-in part of the Ladybug Tools, working inside visual programming environments such as Grasshopper and Dynamo. It supports detailed daylight and solar irradiation simulations using Radiance and energy simulations using EnergyPlus and OpenStudio ([HB]). The study was performed using the improved two-phase Radiance method, available in the Honeybee [+] version of the plug-in.

- Indalux

INDALUX is an open-source software package using RADIANCE as a calculation engine to produce particular images characterizing the urban fabric and sky radiance distributions. Various numerical indicators characterising the access to solar radiation (e.g. solar irradiation) and daylight in urban areas can be visually estimated or precisely calculated by overlaying these particular images. ([IDLX]).

- Ladybug

Ladybug provides climate graphics based on weather files and supports solar radiation studies, view analyses, and sunlight-hours modelling. It is embedded within the visual programming language environment Grasshopper, linked to Rhino3D ([HB]).

- Spacemaker

Spacemaker's photovoltaic analysis is a prototype and is still under active development. However, it will be available to users in a Beta release in the Spacemaker product soon. The photovoltaic analysis uses local solar radiation data and Spacemaker's sun analysis to give users the ability to see the potential of their site for solar panel energy generation at the early phases of design ([Spacemaker]).

## 3. Results

To compare results obtained with the different tools, various levels of complexity will be analysed. First, we will consider the case of an unshaded building, then the case of a homogeneous district and finally the case of a more random distribution of buildings.

### 3.1. Unshaded roof

Unlike the geometry presented in Figure 1, the building considered in this section has no neighbours' buildings around it and, therefore, is not subject to any shadings or reflection from the surrounding built environment, except those from the ground. Hence, these results can be used as a reference to assess the impact of the surrounding geometry on the received solar irradiation. The hourly solar irradiation received on the flat roof in the case of an isolated building is presented for the day of February in Figure 2.

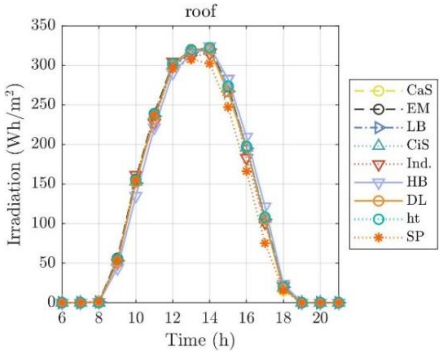


**Figure 2 Hourly irradiation received on the roof in February**

Here all the tools provide similar results. This is expected since in the present case the surface of interest is horizontal without any shadings or potential solar reflections. Therefore, the results should be almost identical to the $G_h$ provided in the weather file. However, it can be observed that results are non-identical. This is mostly due to how each tool handles the input information. Indeed, based on the .epw data dictionary, ("EnergyPlus Weather File (EPW) Data Dictionary: Auxiliary Programs — EnergyPlus 8.3,"), the meteorological quantity provided at the hour *h* corresponds to the integral/average of this quantity over the previous hour. To account for this, some tools shift the sun position by approximately *30 min* before the required hour. Consequently, for a result at hour *h*, the sun position at *h-30min* is sometimes used. However, unless we have total access to the source code, it is sometimes difficult to know whether this shift is done or not in the tool. Furthermore, this correction can be relevant with *epw files*, but it may not be relevant for other input files.

## 3.2. Unshaded facades

The irradiation on the North, West and South façades for the unshaded case is presented in Figure 3. Here it can be observed that the results on the North façades are relatively more sensitive with differences that can reach more than 100% at 1.00 p.m. However, this only represents an absolute difference of 60Wh/m². Given that there is no direct sun on this façade, the observed differences will mainly come from the diffuse model and the reflections. For example, for the present simulations, htrdr used intentionally an isotropic sky which results in a higher predicted irradiation on the North and a lower value on the southern façade. On the other hand, LB tool does not consider reflections, which results in a lower prediction of the solar irradiation. On the southern façades, differences by up to 150 Wh/m$^2$ are observed at 2.00 p.m., which corresponds here to a relative difference of 50%.

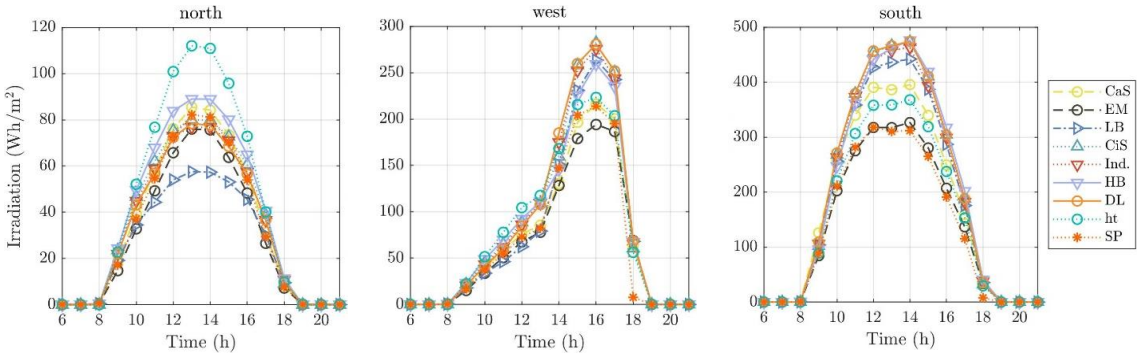


**Figure 3: North, West and South façades fort the unshaded case in February**

## 3.3. Homogeneous district

The spatially averaged hourly irradiation received on the southern façade for the homogeneous district has been plotted in Figure 4 for February (left) and August (right).

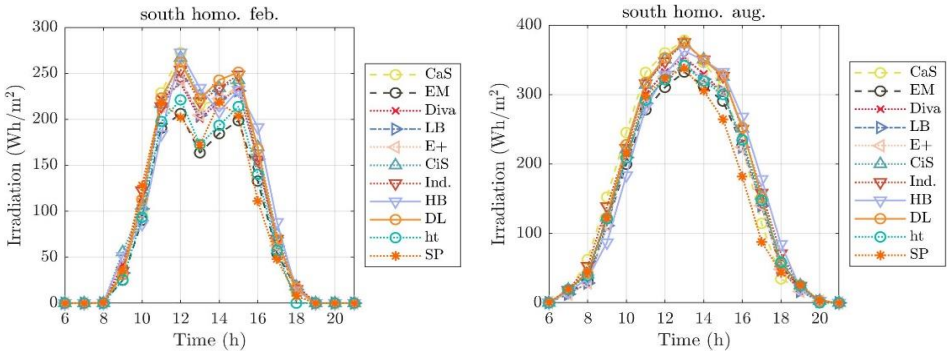


**Figure 4: Irradiation on the southern face of the homogeneous district (left) February, (right) August**

The impact of surrounding buildings can be seen in February since they generate a 'double hump' shape around 1.00 p.m. A maximum absolute difference of 100 Wh/m² is observed at 1.00 p.m. This represents a relative difference of 43% which is less than the maximum relative difference observed in the unshaded case.

## 3.4. Heterogeneous district

For the heterogeneous district (Figure 5) the predictions of the different tools are once again in good agreement. However, in winter, the solar irradiation is more sensitive to the district because of the lower position of the sun. Despite the relatively good agreement, the peaks (minimum or maximum values) are not predicted at the same time. For example, according to SP or Indalux the minimum during the day is reached at 10 a.m. whereas CaS or HB predict it the next hour. Similarly, the second peak is not predicted at the same time by all the tools. Finally, it can also be seen that in this more complex scenario, there is no tool that either provides maximum or minimum results for all timesteps compared to the other tools. For example, at 1.00 p.m., *SP* provides the maximum predicted irradiation, whereas at 2.00 p.m. and 3.00 p.m. it is respectively CaS and HB that predict the highest irradiation.

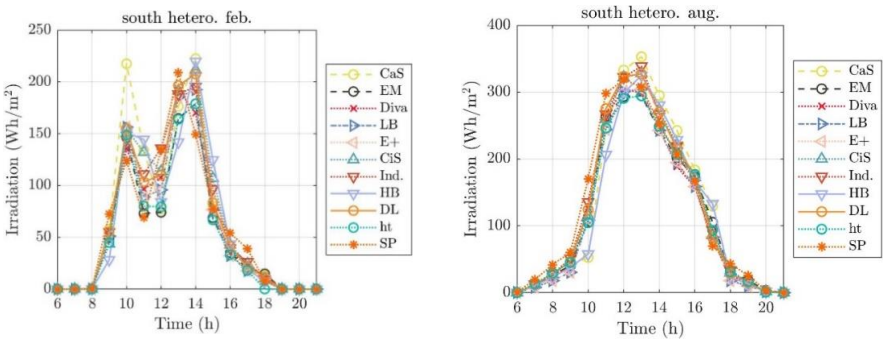


**Figure 5 Irradiation on the southern face of the heterogeneous district (left) February, (right) August**

## 3.5. Prediction variability

To better assess the variation of the results, we define here the variation of hourly irradiation $I(h)$ of the $k^{ith}$ tool by:

$$I'_k(h) = I_k(h) - \frac{1}{N_T}\sum_{n=1}^{N_T} I_n(h) \qquad \text{(eq. 2)}$$

$N_T$ being the number of investigated tools here $N_T = 10$.

The daily evolution of the distribution of $I'_k(h)$ is plotted in Figure 6 for the West façade for the four different scenarios (February, August, homogeneous/heterogeneous). Here the minimum and maximum values of $I'_k(h)$ (defined as $\min/\max(I'_k(h), k \in N_T)$ as well as the 25$^{th}$ and 75$^{th}$ percentile of $I'_k(h)$ are plotted. It can be observed that the difference between the maximum and minimum predicted value can be significant, up to 150 Wh/m². This represents the largest deviation observed in the results.

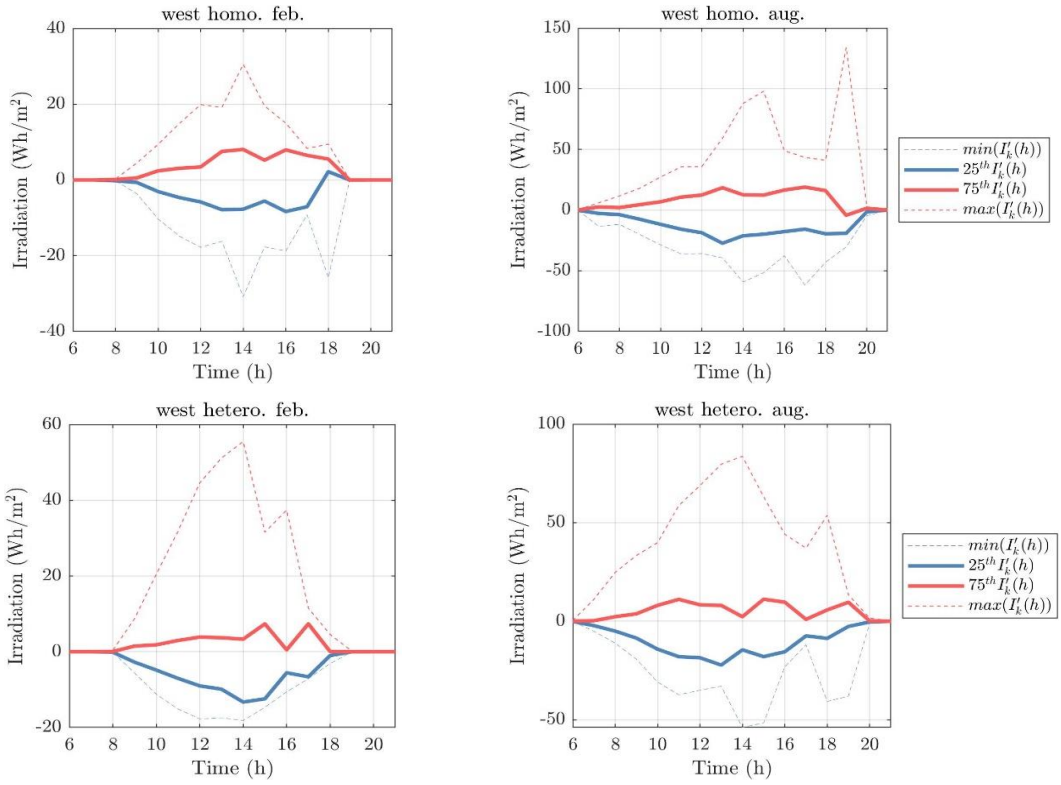


**Figure 6: Evolution of the variation of $I'_k(h)$ during the day for the West façade in the four different scenarios.**

To have a better overview of the variations in the irradiation for all tested configurations, we define a global indicator called the deviation intensity *(DI)*. It is defined here as:

$$DI = \frac{\sum_{h=1}^{24} \sqrt{\sum_{n=1}^{N_t} I'_k(h)^2}}{\sum_{h=1}^{24} \sum_{n=1}^{N_t} I_k(h)}, \qquad \text{(eq. 3)}$$

which can be seen as the daily average of the standard deviation divided by the daily average of the tool-averaged irradiation. This allows scaling the standard deviation by the mean daily irradiation which provides a better insight into the variability between the results (Table 3).

**Table 3: DI values for the different periods and scenario**

| Period of analysis | **February** | | | **August** | | |
|---|---|---|---|---|---|---|
| Scenario | **unshaded** | **homo.** | **hetero.** | **unshaded** | **homo.** | **hetero.** |
| **East** | 17.4 % | 14.0 % | 37.0 % | 17.5 % | 14.5 % | 33.0 % |
| **West** | 14.1 % | 12.9 % | 49.0 % | 13.5 % | 18.1 % | 38.7 % |
| **North** | 17.6 % | 26.0 % | 46.4 % | 24.3 % | 36.0 % | 45.5 % |
| **Roof** | 3.4 % | 3.4 % | 8.3 % | 3.0 % | 3.0 % | 8.4 % |
| **South** | 14.2 % | 10.7 % | 16.8 % | 13.8 % | 7.9 % | 10.0 % |

For the day of February, it should be noted that, except for the North façade, the *DI* is lower for the homogeneous district than for the unshaded building. These results might seem slightly counter-intuitive since by increasing the complexity of the geometry, i.e., by adding buildings to the district, one would expect a higher diversity in the results. In August there are no special trends since, in the homogeneous district, the *DI* is higher for the North and West façade, whereas it is less for the South and East façade.

However, for both the investigated days, the *DI* is significantly higher in the heterogeneous district. This could be explained by two factors:

- The geometry is relatively random, without any symmetries, therefore increasing the complexity of the shadow castings.
- The analysed building (i.e. central building in the heterogeneous district, Figure 1) is small compared to its neighbours. As a result, it is highly shaded by the other buildings. In this case, the impact of the modelling of the reflection and the diffuse components are predominant.

## 3.6. Façade Mapping

One of the issues with the spatial averaging performed for previous figures is that it can erase or smooth some behaviours. To have a better idea of the difference between the tools, the distribution of the irradiation on the façade can be studied. This is illustrated in Figure 7 with the East façade of the homogeneous district in February. The three rows respectively correspond to 9.00 a.m., 10.00 a.m. and 11.00 a.m. As mentioned in sections 2.1 and 2.3, the façade is 30-m high and 20-m long, and the spatial resolution is 1 m².

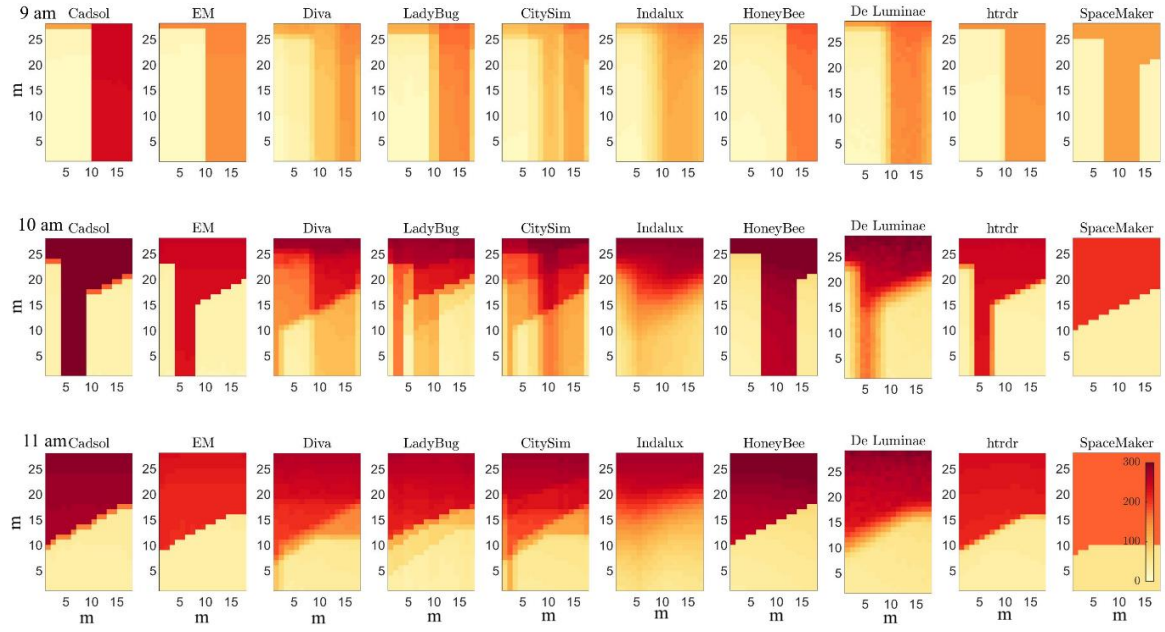


**Figure 7: Distribution of the irradiation at 9.00, 10.00 et 11.00 a.m. (1st, 2nd and 3rd lines). Case of the East façade of the homogeneous district in February. The colour scale, ranges from 0 to 300 Wh/m², displays the hourly irradiation (in Wh/m²)**

First, it can be observed that all tools provide a different distribution of irradiance. Nevertheless, some common features are visible:

- Some tools predict a sharp distribution of solar irradiance. It is here the case of Spacemaker, htrdr, HoneyBee, CadSol and ENVI-met. Indeed, for these tools, it is possible to visualize and localize which parts of the building envelope (façades and roof) are hit by the direct component at the evaluated hour.

However, even between these tools, differences in the shape occurs. This is due to a difference in the sun position. Indeed, depending on when within the hour the sun position is evaluated, the distribution of the direct radiation on the façade is impacted. This is particularly striking when comparing HB, htrdr and SP. Considering the results at 10.00 a.m., htrdr evaluates the sun position 30 min behind the required hour, therefore at 9.30 a.m. Based on that, the shape of the irradiance distributions, suggest that HB evaluates the sun position at a later time, here maybe at 10.00 a.m., whereas SP evaluates it an earlier time, maybe 9.00 a.m.

- A more continuous spatial distribution is observed in Indalux. The reason for this is that Indalux proceeds to a sub-hourly evaluation of the sun path at six intermediate positions within the hour. From this, six distributions of solar irradiances are calculated and averaged to provide the final hourly outcomes.
- It is interesting to observe that there are no significant differences in the distribution of the solar irradiation between tools using radiosity methods (e.g. Cadsol, CitySim, ENVI-met) from those using a ray-tracing approach (htrdr, HB, Diva). However, for all tools, reflections were diffuse. Introducing specular reflections (by adding glass walls for example), could have provided another outcome since classic radiosity approaches cannot account for the incidence angle (and therefore the specular reflections).

## 4. Conclusive remarks

This paper shows a critical comparison of the results obtained with some popular simulation tools for urban solar radiation studies. In total ten tools were studied for three scenarios, an isolated building (Unshaded), a building in an aligned district (Homogeneous), a building in a more random district (Heterogeneous). Each tool simulated the hourly solar irradiation on the envelope (façades and roof), for two representative days, one in August and the other in February.

- One of the striking points of this study is that, for similar input conditions and standard inputs, there are as many different results as tools. However, it should be noted that, despite using the same settings, the instructions sent to the contributors (and co-authors) did not specify an explicit sun position for each hour, which led to possible differences in dealing with the input parameters, notably due to the consideration of the hourly weather data as instantaneous or time-integrated values.
- There are very small variations between the tools outcomes when predicting the solar irradiation received on an unobstructed flat roof. However, predicted solar irradiation can largely vary for the façade, by up to 150 Wh/m² in the present case (40% in relative error).
- No single tool constantly over- or under-estimates hourly spatially-aggregated results with respect to the other tools. This would suggest in principle lower deviations if results were integrated over larger time scales.
- When comparing the relative difference of the mean solar irradiation there are no significant differences in the tools' results between the unshaded and the homogeneous scenarios. However, the deviation in the predicted irradiation significantly increases in the heterogeneous district. The reason is that the heterogeneous district is more complex, and the studied building in this scenario is smaller than its neighbours, and therefore subject to more shading.
- In some specific cases, explanations have been found to observed differences in the predicted solar irradiation (i.e. time at which the sun position is calculated, type of diffuse model, absence of reflection). However, some differences and behaviours remain unexplained, as this would require a more thorough analysis of the backend simulation engine/source code of each tool, which was out of the scope of this paper.

This work finally highlights that, depending on the tool and settings that are used, unneglectable deviations in the hourly results can be expected, especially for complex geometry.

## 5. Acknowledgements

The authors would like to thank the program INTERREG V Suisse- France for providing financial support to conduct this study in the framework of the project G2 Solar, which aims at extending the solar cadaster to the Greater Geneva area and increasing energy solar production at this level. This work has been supported by the HES-SO University of Applied Sciences and Arts Western Switzerland in the framework of the project VALES, as well as has by the French National Research Agency, through the Investments for Future Program (Ref. ANR-18-EURE-0016 - Solar Academy). The research units LOCIE is a member of the INES Solar Academy Research Centre. G.P. acknowledges funding from the European Union's Horizon 2020 research and innovation program under grant agreement N°884161. Thanks to the IEA SHC Task 63 'Solar Neighborhood Planning' that provided the framework to gather the expertise required to achieve such work.

## 6. References

Desthieux, G., Carneiro, C., Camponovo, R., Ineichen, P., Morello, E., Boulmier, A., Abdennadher, N., Dervey, S., Ellert, C., 2018. Solar Energy Potential Assessment on Rooftops and Facades in Large Built Environments Based on LiDAR Data, Image Processing, and Cloud Computing. Methodological Background, Application, and Validation in Geneva (Solar Cadaster). Front. Built Environ. 4. https://doi.org/10.3389/fbuil.2018.00014

[DL-LIGHT], n.d. Index, Welcome to DL-Light, Extension study daylit ambiance within SketchUp [WWW Document]. URL https://deluminaelab.com/dl-light/en/ (accessed 10.16.21).

[E+], n.d. EnergyPlus Weather File (EPW) Data Dictionary: Auxiliary Programs — EnergyPlus 8.3 [WWW Document]. URL https://bigladdersoftware.com/epx/docs/8-3/auxiliary-programs/energyplus-weather-file-epw-data-dictionary.html (accessed 10.14.21).

Freitas, S., Brito, M.C., 2019. Solar façades for future cities. Renewable energy focus 31, 73–79. https://doi.org/10.1016/j.ref.2019.09.002

Govehovitch, B., Thebault, M., Bouty, K., Giroux-Julien, S., Peyrol, É., Guillot, V., Ménézo, C., Desthieux, G., 2021. Numerical validation of the radiative model for the solar cadaster developed for greater Geneva. Applied Sciences 11, 8086. https://doi.org/10.3389/fbuil.2018.00014

[HB], n.d. Ladybug Tools | Home Page [WWW Document]. URL https://www.ladybug.tools/ (accessed 10.16.21).

[htrdr], n.d. |M|S> htrdr [WWW Document]. URL https://www.meso-star.com/projects/htrdr/man/man1/htrdr.1.html (accessed 10.16.21).

[IDLX], n.d. [IDLX] [WWW Document]. URL https://phybat.heia-fr.ch/idlx/ (accessed 10.16.21).

IRENA, 2019. Future of Solar Photovoltaic: Deployment, investment, technology, grid integration and socio-economic aspects (A Global Energy Transformation: paper). International Renewable Energy Agency.

Klein, S.A., 1977. Calculation of monthly average insolation on tilted surfaces. Solar Energy 19, 325–329. https://doi.org/10.1016/0038-092X(77)90001-9

Natanian, J., Aleksandrowicz, O., Auer, T., 2019. A parametric approach to optimizing urban form, energy balance and environmental quality: The case of Mediterranean districts. Applied Energy 254, 113637. https://doi.org/10.1016/j.apenergy.2019.113637

Peronato, G., Rey, E., Andersen, M., 2018. 3D model discretization in assessing urban solar potential: the effect of grid spacing on predicted solar irradiation. Solar Energy 176, 334–349. https://doi.org/10.1016/j.solener.2018.10.011

Reinhart, C.F., Walkenhorst, O., 2001. Validation of dynamic RADIANCE-based daylight simulations for a test office with external blinds. Energy and Buildings 33, 683–697. https://doi.org/10.1016/S0378-7788(01)00058-5

Robinson, D., Stone, A., 2005. A simplified radiosity algorithm for general urban radiation exchange. Building

Services Engineering Research and Technology 26, 271–284. https://doi.org/10.1191/0143624405bt133oa

Simon, H., Sinsel, T., Bruse, M., 2021. Advances in Simulating Radiative Transfer in Complex Environments. Applied Sciences 11, 5449. https://doi.org/10.3390/app11125449

[Spacemaker], n.d. Spacemaker - AI Architecture Design | Building Information Modelling [WWW Document]. URL https://www.spacemakerai.com// (accessed 10.19.21).

TASK63, n.d. IEA SHC || Task 63 || Solar Neighborhood Planning [WWW Document]. URL https://task63.iea-shc.org/ (accessed 10.18.21).